Since January 2020 Elsevier has created a COVID-19 resource centre with free information in English and Mandarin on the novel coronavirus COVID-19. The COVID-19 resource centre is hosted on Elsevier Connect, the company's public news and information website.

Elsevier hereby grants permission to make all its COVID-19-related research that is available on the COVID-19 resource centre - including this research content - immediately available in PubMed Central and other publicly funded repositories, such as the WHO COVID database with rights for unrestricted research re-use and analyses in any form or by any means with acknowledgement of the original source. These permissions are granted for free by Elsevier for as long as the COVID-19 resource centre remains active.

Protein Expression and Purification 116 (2015) 19–29

Contents lists available at ScienceDirect

Protein Expression and Purification

journal homepage: www.elsevier.com/locate/yprep

Structural characterization by transmission electron microscopy and immunoreactivity of recombinant Hendra virus nucleocapsid protein expressed and purified from *Escherichia coli*

Lesley A. Pearce [a,*], Meng Yu [b], Lynne J. Waddington [a], Jennifer A. Barr [b], Judith A. Scoble [a], Gary S. Crameri [b], William J. McKinstry [a]

[a] CSIRO Manufacturing Flagship, Parkville, Victoria, Australia
[b] CSIRO Australian Animal Health Laboratory and Biosecurity Flagship, Geelong, Victoria, Australia

ARTICLE INFO

Article history:
Received 12 June 2015
and in revised form 15 July 2015
Accepted 16 July 2015
Available online 18 July 2015

Keywords:
Hendra virus
Nucleocapsid
Recombinant protein expression
Purification
Electron microscopy
Luminex assay

ABSTRACT

Hendra virus (family *Paramyxoviridae*) is a negative sense single-stranded RNA virus (NSRV) which has been found to cause disease in humans, horses, and experimentally in other animals, e.g. pigs and cats. Pteropid bats commonly known as flying foxes have been identified as the natural host reservoir. The Hendra virus nucleocapsid protein (HeV N) represents the most abundant viral protein produced by the host cell, and is highly immunogenic with naturally infected humans and horses producing specific antibodies towards this protein.

The purpose of this study was to express and purify soluble, functionally active recombinant HeV N, suitable for use as an immunodiagnostic reagent to detect antibodies against HeV. We expressed both full-length HeV N, (HeV N_{FL}), and a C-terminal truncated form, (HeV N_{CORE}), using a bacterial heterologous expression system. Both HeV N constructs were engineered with an N-terminal His_{x6} tag, and purified using a combination of immobilized metal affinity chromatography (IMAC) and size exclusion chromatography (SEC). Purified recombinant HeV N proteins self-assembled into soluble higher order oligomers as determined by SEC and negative-stain transmission electron microscopy. Both HeV N proteins were highly immuno-reactive with sera from animals and humans infected with either HeV or the closely related Nipah virus (NiV), but displayed no immuno-reactivity towards sera from animals infected with a non-pathogenic paramyxovirus (CedPV), or animals receiving Equivac® (HeV G glycoprotein subunit vaccine), using a Luminex-based multiplexed microsphere assay.

Crown Copyright © 2015 Published by Elsevier Inc. All rights reserved.

1. Introduction

Emerging infectious diseases (EIDs) are a constantly evolving threat and a significant burden on public health and the global economy. In today's transient society, EIDs represent a serious public health concern due to their high potential to cause widespread epidemics and pandemics. EID events are dominated by zoonoses (>60%), characterized by "species-jumping pathogens", the majority of which originate in wildlife and are able to replicate in humans [1]. The most pathogenic of the zoonotic diseases are those caused by RNA viruses, which have an unmatched ability to replicate in the new host species' cytoplasm [2,3]. Bats have been identified or implicated as the natural host reservoir for an increasing number of new and often deadly zoonotic viruses [4,5]. Examples of such bat-borne zoonotic diseases include Rift Valley fever virus, severe acute respiratory syndrome coronavirus

Abbreviations: CedPV, Cedar virus; EIDs, emerging infectious diseases; ESI-TOF-MS, electro-spray ionization time-of-flight mass spectrometry; HeV, Hendra virus; HeV N, Hendra virus nucleocapsid protein; HeV N_{FL}, Hendra virus nucleocapsid protein (full length, amino acid residues 1–532); HeV N_{CORE}, Hendra virus nucleocapsid protein CORE region (amino acid residues 1–402); IDR, intrinsically disordered region; IMAC, immobilized metal affinity chromatography; IPTG, isopropyl-β-D-thiogalactopyranoside; L, Hendra virus RNA polymerase; MERS-CoV, Middle East respiratory syndrome coronavirus; MeV, Measles virus; N-RNA, Hendra virus nucleocapsid protein complexed with viral RNA; NiV, Nipah virus; NiV N, Nipah virus nucleocapsid protein; N, nucleocapsid; nsNSRV, non-segmented negative-sense single-stranded RNA virus; P, phosphoprotein; RNP, ribonucleocapsid protein complex; SARS-CoV, Severe acute respiratory syndrome coronavirus; SDS–PAGE, sodium dodecyl sulfate polyacrylamide gel electrophoresis; SEC, size exclusion chromatography; sG, soluble G glycoprotein; TBS, TRIS-buffered saline; TEM, transmission electron microscopy.

* Corresponding author at: CSIRO Manufacturing Flagship, 343 Royal Parade, Parkville, Victoria 3052, Australia.
E-mail address: lesley.pearce@csiro.au (L.A. Pearce).

http://dx.doi.org/10.1016/j.pep.2015.07.008
1046-5928/Crown Copyright © 2015 Published by Elsevier Inc. All rights reserved.

(SARS-CoV) and Middle East respiratory syndrome coronavirus (MERS-CoV), Japanese Encephalitis virus, Ebola filovirus, Rabies lyssavirus, and the *Paramyxoviridae* including Hendra and Nipah virus [6].

In 1994, Hendra virus (HeV) was first described as the causative agent for an outbreak of a severe and fatal respiratory disease occurring in horses in Northern Australia, followed by the fatal transmission of the disease to two humans working in close contact with these animals [4,7–9]. Since then there has been more than 48 sporadic Hendra virus outbreaks in Australia, killing four of the seven humans known to be infected with the virus and many horses [9]. In 1998, a deadly outbreak of respiratory disease in pigs and abattoir workers in Malaysia was caused by the very closely related henipavirus species, Nipah virus (NiV) [4,9–13]. Outbreaks of NiV continue to occur throughout South-East Asia, India and Bangladesh. Both HeV and NiV are highly pathogenic in a wide variety of mammals, with mortality rates approaching 60%. Symptoms include; pulmonary hemorrhage and edema, encephalitis and meningitis.

A number of pteropid bat species, including flying foxes (fruit bats) have been identified as the natural wildlife reservoir for dispersing HeV and NiV [6]; however, these animals tend to be asymptomatic when infected with the virus and little is known about the factors that trigger viral spill-over to humans or other animals. Our colleagues have recently identified the existence of a closely related, but non-pathogenic henipavirus; Cedar virus (CedPV), which is also transmitted by pteropid bat species [14]. Laboratory studies utilizing guinea pigs have demonstrated that CedPV can replicate in these animals, develop neutralizing antibodies, but remain clinically well [14]. The absence of therapeutic treatments for HeV and NiV, together with the susceptibility of humans to both viruses and their high virulence, has led to the classification of HeV and NiV as Biosafety Level 4 (BSL-4) pathogens [8,9,15]. A vaccine for HeV (Equivac®) has recently been developed for use in horses that is effective at protecting them from HeV infection, breaking the only known transmission mechanism from bats to humans [9,16–18].

HeV and NiV are members of the genus *Henipavirus*, and belong to the RNA virus family *Paramyxoviridae*, order *Mononegavirales* (non-segmented negative sense single-stranded RNA viruses (nsNSRV)). The close relatedness of both HeV and NiV is further demonstrated by the observation that antibodies produced against one virus can neutralize the other in serum neutralization assays, albeit with reduced efficiency [16]. The genomic RNA from HeV and NiV along with other nsNSRV (e.g. Measles virus) encodes the six major viral structural proteins; nucleocapsid protein (N), phosphoprotein (P), matrix protein (M), fusion protein (F), attachment glycoprotein (G), and the large protein (L) (RNA polymerase) [8,11,19,20], the most abundant protein being the N protein [21–23]. The size of both the HeV genome (18.234 kilobases) and NiV genome (18.246 kilobases) are considerably larger than other paramyxoviruses (average size 15.6 kilobases), and fit the "rule of six", which stipulates that the paramyxovirus RNA polymerase will only replicate efficiently if the viral genome is a multiple of six nucleotides (6n + 0 nucleotides) [20,24,25]. Interestingly, the length of these genomes is somewhat closer to the length of the genomes of family *Filoviridae viruses* (18.9–19.1 kilobases), which includes Ebola and Marburg viruses [26,27]. The N protein of NSRV forms a complex with viral RNA (N-RNA), which then associates with P and L to form a stable ribo-nucleocapsid protein complex (RNP) required for the transcription and replication of viral RNA [28,29].

The C-terminal region of recombinant NiV N is the most immuno-reactive domain of this protein. Previous studies have indicated that only the C-terminal region of a series of deletion mutants of NiV N was recognized by sera from humans and pigs naturally infected with NiV [23]. In this study, we have expressed and purified recombinant full-length HeV N (HeV N_{FL}) and a C-terminally truncated form, HeV N_{CORE} using an *Escherichia coli* protein expression system. Both recombinant HeV N proteins self-assembled into the classic morphological RNP structures previously observed with other recombinant paramyxovirus N proteins in the absence of viral genomic RNA and viral proteins. Furthermore, both recombinant HeV N proteins were immuno-reactive with sera from HeV and NiV naturally or laboratory infected humans and animals.

2. Materials and methods

2.1. Bacterial strains and media

All transformation steps were carried out using the *E. coli* strains XL1 Blue F′ and BL21 AI using chemical or electro-competent cells and standard procedures. The production of plasmid DNA was in XL1 Blue F′ cells and the production of recombinant protein in BL21 AI, cells were cultured in 2× YT Medium [1.6% (w/v) tryptone, 1.0% (w/v) yeast extract, and 0.5% NaCl] or Terrific Broth [1.2% (w/v) tryptone, 2.4% (w/v) yeast extract, 0.4% glycerol buffered with 1/10th volume of 0.17 M KH_2PO_4, 0.72 M K_2HPO_4], respectively. The media was supplemented with 100 μg/mL ampicillin for both XL1 Blue F′ and BL21 AI.

2.2. Plasmid construction

Viral genomic RNA was extracted from inactivated virus pellet using QIAamp Viral RNA Mini Kit (Qiagen). The TimeSaver cDNA synthesis kit (Pharmacia) was used to make total cDNA using random hexamer primers. The construction of fusion protein expression plasmids has been described previously [19,30]. Briefly, the HeV N_{FL} gene coding sequence (amino acids residues 1–532; GenBank: AAC83187.1) was amplified directly by PCR from cDNA template with forward primer 5′-TTCAAGATCTCAAAATGAGTGATATATT-3′ and reverse primer (5′-CTCTTGAATTCATTTATAAGAGTGTGTC-3′ with the underlined regions representing recognition sites for the restriction endonucleases *Bgl*II and *Eco*RI respectively. The PCR product of HeV N fragment was purified through QIAquick PCR Purification kit (Qiagen) and digested with *Bgl*II and *Eco*RI under standard conditions and ligated using T4 DNA ligase (Promega) into the linearized T7 expression vector pRSET-C (Life Technologies) previously digested with the same two enzymes [31]. The HeV N_{CORE} coding sequence (amino acid residues 1–402; GenBank: AAC83187.1) was chemically synthesized as an *E. coli* codon-optimized sequence (GeneArt®, Life Technologies). *Bam*HI and *Nhe*I restriction endonuclease sites were engineered at the 5′ and 3′ ends of the HeV N_{CORE} coding sequence to facilitate cloning into a pET43.1a (Novagen) protein expression vector that we had previously modified. This modified pET43.1a protein expression vector had the 5′ NusA and S tags replaced with a His_{x6} tag, and the Enterokinase and Thrombin protease cleavage sites replaced with a TEV protease cleavage site followed by a 5′ *Bam*HI and 3′ *Nhe*I restriction sites to facilitate gene cloning. The HeV N_{CORE} pET43.1a expression plasmid was verified by DNA sequencing.

2.3. Analytical protein expression studies

Small-scale recombinant protein expression studies were performed by inoculating a single colony into 10 mL 2× YT media containing ampicillin (100 μg/mL) and glucose (2.0%) overnight at 37 °C, with shaking at 160 rpm. The overnight cultures were used

to inoculate 10 mL fresh 2× YT media (HeV N_{FL}) or Terrific Broth (HeV N_{CORE}) containing ampicillin (100 μg/mL) and glucose (0.1%) at a starting OD_{600nm} of 0.1 and the culture was grown at 37 °C, 160 rpm, until an OD_{600nm} of 0.5 was reached, at which point the temperature was reduced to 26 °C for HeV N_{FL} and 18 °C for HeV N_{CORE}. At an OD_{600nm} of 0.8, the expression of both HeV N constructs was induced by the addition of 1.0 mM isopropyl-β-D-thiogalactopyranoside (IPTG, GoldBio) and 0.25% arabinose (Sigma–Aldrich) and protein expression monitored over a 20 h period by the collection of 200 μL culture aliquots at $T = 0$, 4, and 20 h post-induction. The cells were harvested by centrifugation at 14,000 rpm for 5 min and then frozen. Bacterial cell pellets were solubilized by incubation in 80 μL of His A buffer (20 mM sodium phosphate buffer, pH 7.5 containing 500 mM NaCl, and 20 mM imidazole) supplemented with 2 mM $MgCl_2$, 0.25 mg/mL lysozyme and 25 U/mL Benzonase® (Merck Millipore) followed by three freeze–thaw cycles and incubation at 37 °C for 20 min. To separate the soluble protein fraction from the insoluble fraction, the lysate was centrifuged at 14,000 rpm for 5 min. The soluble protein supernatant was removed and the remaining insoluble pellet was resuspended in 80 μL of 8 M urea. Soluble and insoluble time-course samples were mixed with 4× LDS SB (Life Technologies) for analysis by SDS–PAGE and Western blotting.

2.4. Large-scale protein production

Large-scale recombinant protein production was performed by inoculating a single colony into 150 mL 2× YT media containing ampicillin (100 μg/mL) and glucose (2.0%), and cultured at 37 °C, overnight with shaking at 200 rpm. The overnight culture was used to inoculate 1.0 L media containing antibiotics in a 2.5 L baffled plastic Erlenmeyer flask [HeV N_{FL} (2× YT media) and HeV N_{CORE} (Terrific Broth)]. The cultures were grown at 37 °C, 200 rpm, until an OD_{600nm} of approximately 0.5 was reached and the temperature was reduced to 26 °C (HeV N_{FL}) and 18 °C (HeV N_{CORE}). At an OD_{600nm} of 0.8 protein expression was induced with the addition of 1 mM IPTG (GoldBio) and 0.25% arabinose (Sigma–Aldrich) and the cells grown for a further 4 h at 26 °C (HeV N_{FL}) or 20 h at 18 °C (HeV N_{CORE}). Cells were harvested by centrifugation (6000 rpm, 4 °C, 15 min), and cell pellets stored at −80 °C.

Cell pellets (50 g) were resuspended in 500 mL ice cold His A buffer [20 mM sodium phosphate buffer, pH 7.5, containing 500 mM NaCl and 20 mM imidazole] containing 50 mg lysozyme (Sigma–Aldrich), 2 mM PMSF (Sigma–Aldrich), five EDTA-Free cOmplete Protease inhibitor tablets (Roche) and 2500 Units Benzonase®(Merck Millipore). Additional protease inhibitors were added to the lysis buffer for HeV N_{FL}: 2 mM AEBSF PefaBloc (Roche), 2 mg/mL Benzamadine (Sigma–Aldrich), 2 μg/mL Aprotinin (GoldBio). Following resuspension, the *E. coli* cells were ruptured by passage three times through an EmulsiFlex-C5 cell homogenizer, (15,000 psi at 4 °C, Avestin) and centrifuged (Beckman JA 16.250, 12,000 rpm, 15 min, 4 °C). The lysate was then loaded at 2.5 mL/min onto a 5 mL IMAC column (HisTrapFF, GE Healthcare) that had previously been equilibrated with His A buffer. The column was washed with 20 mM sodium phosphate buffer, pH 7.5, containing 500 mM NaCl and 40 mM imidazole to remove weakly bound proteins, and HeV N proteins were eluted with step gradients of His A buffer containing 300 and 500 mM imidazole.

Fractions eluted from the IMAC column containing HeV N were pooled and concentrated using a centrifugal Ultra-15, 10,000 molecular weight cut-off membrane (Merck Millipore). The concentrated protein was then fractionated by SEC using a HiLoad 26/600 Superdex 200 pg column (GE Healthcare) for HeV N_{FL} and a HiLoad 16/600 Superdex 200 pg column (GE Healthcare) for HeV N_{CORE}. These columns were previously equilibrated in 50 mM Tris buffer, pH 7.5, containing 500 mM NaCl and 5% glycerol. Peak fractions containing either HeV N_{FL} or HeV N_{CORE} proteins were pooled and then concentrated and frozen in liquid nitrogen before storage at −80 °C.

2.5. SDS–polyacrylamide gel electrophoresis and Western blotting

Analytical expression studies and the large scale production of recombinant HeV N were monitored by both SDS–PAGE and Western blotting under reducing conditions on 4–12% Bis–Tris NuPAGE gels (Life Technologies) using MES electrophoresis buffer. Samples were incubated with SDS sample buffer and heated to 95 °C for 5 min prior to loading onto gels. Protein gels were stained with Coomassie Brilliant Blue. Replicate gels were transferred onto a nitrocellulose membrane for Western blotting. The membrane was blocked in phosphate-buffered saline containing 5% (w/v) skim milk powder for 30 min, followed by incubation with an anti-polyHistidine Peroxidase Conjugate antibody (A7058, Sigma–Aldrich) to detect His_{x6}-tagged proteins. The membranes were washed several times with phosphate-buffered saline containing 0.05% Tween-20 (v/v) before being developed using the chromogenic substrate α-chloronaphthol (Sigma–Aldrich).

2.6. Mass spectrometry

Purified HeV N_{FL} and HeV N_{CORE} were desalted by reverse-phase HPLC (Dionex UltiMate 3000 HPLC) using a C18 Jupiter column (Phenomenex), and the proteins eluted directly onto a microTOF-QII electrospray ionization mass spectrometer (Bruker) using a gradient of acetonitrile containing 0.1% formic acid. The mass of the resulting peaks were determined by maximum entropy-based deconvolution algorithms.

2.7. Electron microscopy analysis

Carbon-coated 300-mesh copper grids were glow-discharged in nitrogen to render the carbon film hydrophilic. A 4 μL aliquot of each HeV N protein (0.03 mg/mL) was pipetted onto separate grids. After a 30 s adsorption time, excess liquid was drawn off using Whatman 541 filter paper, a 5 μL water wash applied, followed by staining with 2% phosphotungstic acid for 10 s. Grids were air-dried before use. The samples were examined using a Tecnai 12 Transmission Electron Microscope (FEI, Eindhoven, The Netherlands) at an operating voltage of 120 KV. Images were recorded using either a Megaview III CCD camera and AnalySIS camera control software (Olympus), or a FEI Eagle 4k × 4k CCD camera. Measurements were made using ImageJ software (http://rsb.info.nih.gov/ij/).

2.8. Luminex assay

Microsphere coupling was carried out using 20 μg of HeV N_{FL} or HeV N_{CORE} coupled to 1×10^6 carboxylated MagPlex® microspheres (Luminex Corporation) using the standard coupling procedure [32]. Control microspheres for HeV, NiV and CedPV soluble-glycoproteins (sG) were coupled by the same method and the assay carried out as described [32]. Briefly, the assay was performed in 96-well micro-titre plates where 1000 coupled microspheres were added to each test well. The beads were blocked with 2% skim milk and mixed with the test sera diluted 1:100 in phosphate-buffed saline containing 0.05% Tween-20 (Sigma–Aldrich). The bound antibodies were then detected using biotinylated Protein A (Pierce) and biotinylated Protein G (Pierce) and streptavidin–phycoerythrin (Qiagen). The beads were interrogated by the lasers in a BioPlex® 200 suspension array system

(BioRad) and the results recorded as the median fluorescent intensity (MFI) of 100 beads.

2.9. Animal sera

All normal control sera were generated from healthy individuals. The horse natural infection sera were obtained from horses infected in the field in Queensland, the exact time post-infection was uncertain, however, the animals were recovering from the acute disease prior to euthanasia. Experimental horse sera were from animals infected with HeV at AAHL and euthanized 9 days post-infection. Vaccinated horses were prepared by intramuscular (IM) injection of Equivac® HeV vaccine (Zoetis). Day 0 sera was taken prior to injection and day 42 sera was taken 42 days post the initial vaccination. Human HeV positive serum was derived from an infected human patient. Positive NiV pig antiserum was generated from a laboratory infection and taken 21 days post-infection. Rabbit recombinant HeV N antiserum was derived from a rabbit injected IM with 3 doses of HeV N protein with serum harvested 7 days after the third injection.

3. Results

3.1. Expression and purification of recombinant HeV N_{FL} and HeV N_{CORE}

The plasmids pRC-HeV N_{FL} and pET43a-HeV N_{CORE} (Fig. 1) were transformed into *E. coli* BL21 AI for recombinant HeV N production. Protein expression was induced with the addition of 1.0 mM IPTG and 0.25% arabinose at 26 °C (HeV N_{FL}) and 18 °C (HeV N_{CORE}). The expressed proteins were analyzed at 4 and 20 h post-induction by SDS–PAGE and Western blotting.

A Coomassie Blue-stained protein band was observed migrating with an apparent molecular weight of ~63 kDa which corresponded to the molecular weight expected for HeV N_{FL}. This band was present at both 4 and 20 h time points in both soluble and insoluble fractions (Fig. 2A). The identity of this band was confirmed by Western blotting using an anti-polyHistidine Peroxidase Conjugate antibody (Fig. 2B). Increasing the time of protein expression to 20 h did not contribute to higher levels of soluble protein production, but resulted in increased levels of proteolysis and the formation of insoluble HeV N_{FL}. As a result of these analytical experiments, a 4 h induction at 26 °C was chosen for optimal HeV N_{FL} protein production.

There was no detectable expression of the HeV N_{CORE} (at the expected molecular weight of ~46.5 kDa) on a Coomassie Blue-stained gel in either the soluble or insoluble fractions for both 4 and 20 h post-induction time points (Fig. 2C). Western blotting of a replicate gel using the anti-polyHistidine Peroxidase Conjugate antibody revealed a faint band of the correct molecular weight in the soluble fraction from the 20 h time point, although the majority of this protein was found to be in the insoluble fraction at 20 h (Fig. 2D).

Large-scale protein expression of recombinant HeV N_{FL} and HeV N_{CORE} was undertaken at 26 °C or 18 °C respectively, protein expression was induced with the addition of 1.0 mM IPTG and 0.25% arabinose, and cells harvested by centrifugation at 4 h post-induction for HeV N_{FL} and 20 h post-induction for HeV N_{CORE}. Both recombinant HeV N_{FL} and HeV N_{CORE} were purified

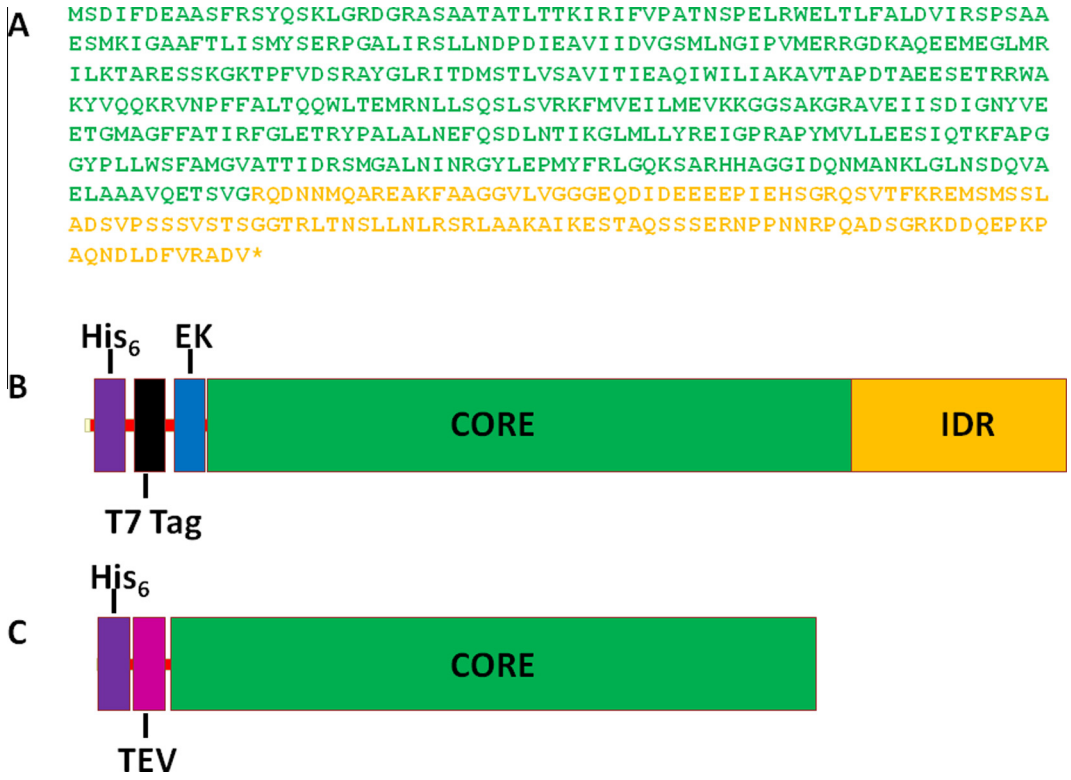

Fig. 1. HeV nucleocapsid protein. (A) Full-length coding sequence for the HeV nucleocapsid protein. (GenBank: AAC83187.1); HeV N CORE domain (amino acid residues 1–402 – green); HeV N Intrinsically Disordered Region (IDR) (amino acid residues 403–532 – orange). (B) Schematic diagram of the full-length HeV nucleoprotein (HeV N_{FL}) construct in *E. coli* expression vector pRC. Polyhistidine region (N-terminal His_{x6} affinity purification tag); T7 tag peptide – MASMTGGQQMG; enterokinase cleavage site – DDDDK; coding sequence for HeV N, HeV N CORE domain (amino acid residues 1–402 – green); HeV N Intrinsically Disordered Region (IDR) (amino acid residues 403–532 – orange). (C) Schematic diagram of the C-terminally truncated HeV N construct (HeV N_{CORE}) in *E. coli* expression vector pET-43a.1. Polyhistidine region (N-terminal His_{x6} affinity purification tag); TEV cleavage site; coding sequence HeV N CORE domain (amino acids 1–402 – green). (For interpretation of the references to color in this figure legend, the reader is referred to the web version of this article.)

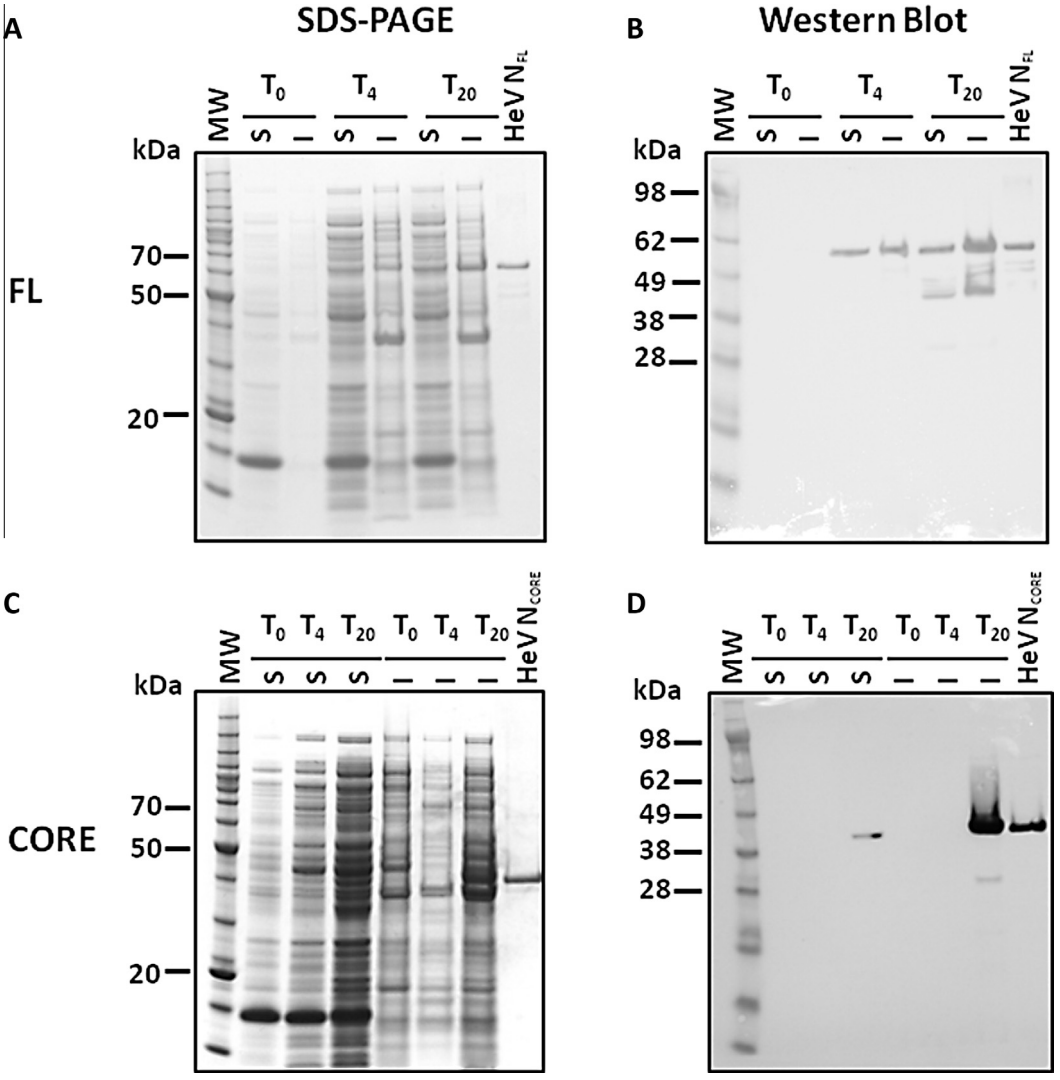

Fig. 2. Analytical expression of recombinant HeV N_{FL} and HeV N_{CORE} in *E. coli* BL21 AI. Bacterial expression samples at $T = 0, 4, 20$ h post-induction on Coomassie Blue-stained SDS–PAGE gels of HeV N_{FL} (A) and HeV N_{CORE} (C). Western blots of duplicate gels of HeV N_{FL} (B) and HeV N_{CORE} (D) transferred onto nitrocellulose and probed with a mouse monoclonal anti-His-HRP conjugated antibody. Soluble (S) and insoluble (I) protein pellet fractions were analyzed. His_{x6}-tagged HeV N_{FL} and HeV N_{CORE}, previously purified under the same conditions as described in the manuscript were included as positive controls.

using a combination of IMAC and SEC under non-denaturing conditions in the presence of 500 mM NaCl and 5% glycerol to minimize protein aggregation and precipitation. Both recombinant HeV N_{FL} and HeV N_{CORE} eluted from the Nickel IMAC column with 300 mM imidazole, were concentrated and further fractionated by SEC. A 1 mg/mL solution of Blue Dextran (Mw 2,000 kDa, High Molecular Weight Gel Filtration Calibration Kit, 28-4038-42, GE Healthcare) in 50 mM Tris, pH 7.5 containing 1 M NaCl was used to determine the void volume of the SEC columns (data not shown). Both HeV N proteins migrated in the calculated void volume of the column (Superdex 200 26/600 gel filtration column V_o – 120.5 mL and Superdex 200 16/600 gel filtration column – V_o 43.6 mL), with an apparent molecular weight of >670 kDa (Fig. 3A and B respectively). This observation was consistent with both proteins forming higher order soluble oligomers. Western blotting using the anti-polyHistidine Peroxidase Conjugate antibody confirmed peak fractions eluting near the void volume were the His_{x6}-tagged HeV N proteins (Fig. 4B and D). Western blot analysis of HeV N_{FL} indicated that the major dominant band was the full-length protein (~65 kDa), this was susceptible to proteolysis in *E. coli* (Fig. 4B). Four C-terminally truncated forms of HeV N were identified by the anti-His-HRP antibody which identified the N-terminal His_{x6} tag on the protein. It is interesting to note that one of the smaller protease resistant fragments of HeV N_{FL} migrated with an apparent molecular weight of 40 kDa (Fig. 4B), which was very similar to the expected size of our expressed HeV N_{CORE} (Fig. 4D).

The gel filtration profile of the HeV N proteins was monitored at two wavelengths; 260 and 280 nm (A_{260} and A_{280}) to enable us to simultaneously observe the nucleic acid and protein profiles of the preparation. The peaks which registered a high level of absorbance at 260 nm were the peaks from the chromatograms (Fig. 3A and B) containing fractions identified on the Western blots as containing His_{x6} tagged protein (Fig. 4B and D). The high level of absorbance at 260 nm indicates the presence of heterologous nucleic acids from *E. coli*, which have been purified in association with both the full-length and C-terminally truncated form of HeV N.

The HeV N_{FL} fractions were pooled and concentrated to 2.5 mg/mL before freezing in liquid nitrogen. We reproducibly obtained 4.8 mg of purified HeV N_{FL} from 6 × 1.0 L cultures grown in 2.5 L shake flasks with a yield of 0.8 mg/L of culture. The purified HeV N_{FL} could be concentrated to between 1 and 2.5 mg/mL in the presence of 500 mM NaCl and 5% glycerol using a centrifugal

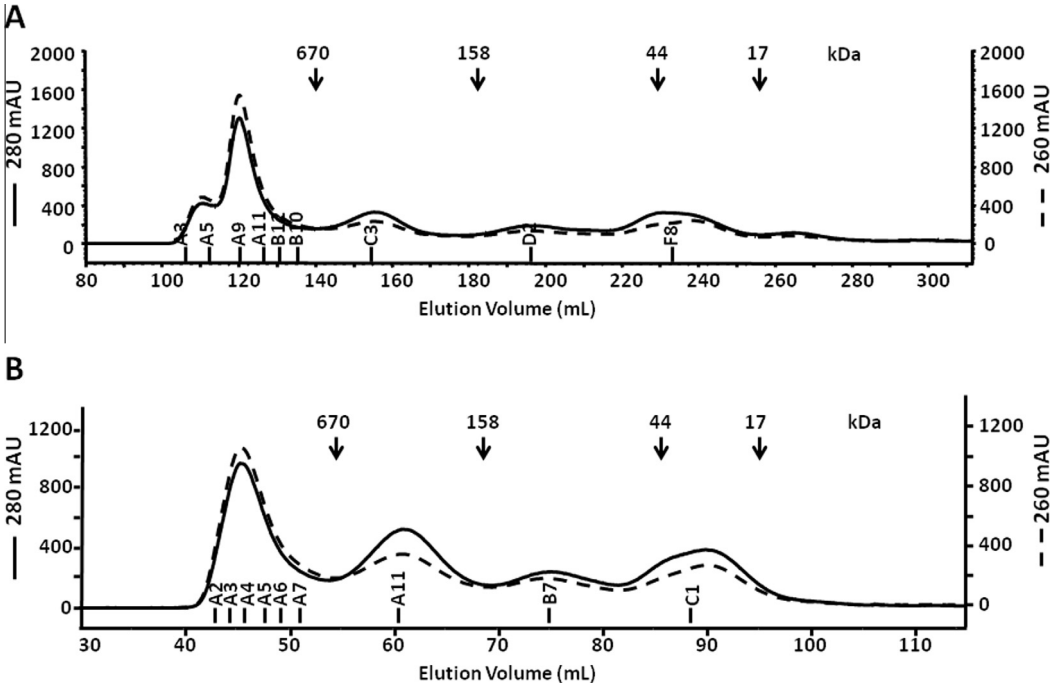

Fig. 3. Size exclusion chromatography of HeV N constructs. Preparative scale size exclusion chromatography (SEC) purification of IMAC purified HeV N. (A) HeV N_{FL} fractionated on Superdex 200 26/600 gel filtration column and (B) HeV N_{CORE} fractionated on a Superdex 200 16/600 gel filtration column. Columns were run in 50 mM Tris, pH 7.5 containing 500 mM NaCl and 5% glycerol. The elution profile indicated a major peak with an apparent molecular weight of greater than 670 kDa, corresponding to high order oligmers of HeV N. The molecular weights (in kDa) of the gel filtration standards used for calibration are indicated at their integrated elution volume. The absorbance of the sample is measured at both A_{280} and A_{260}.

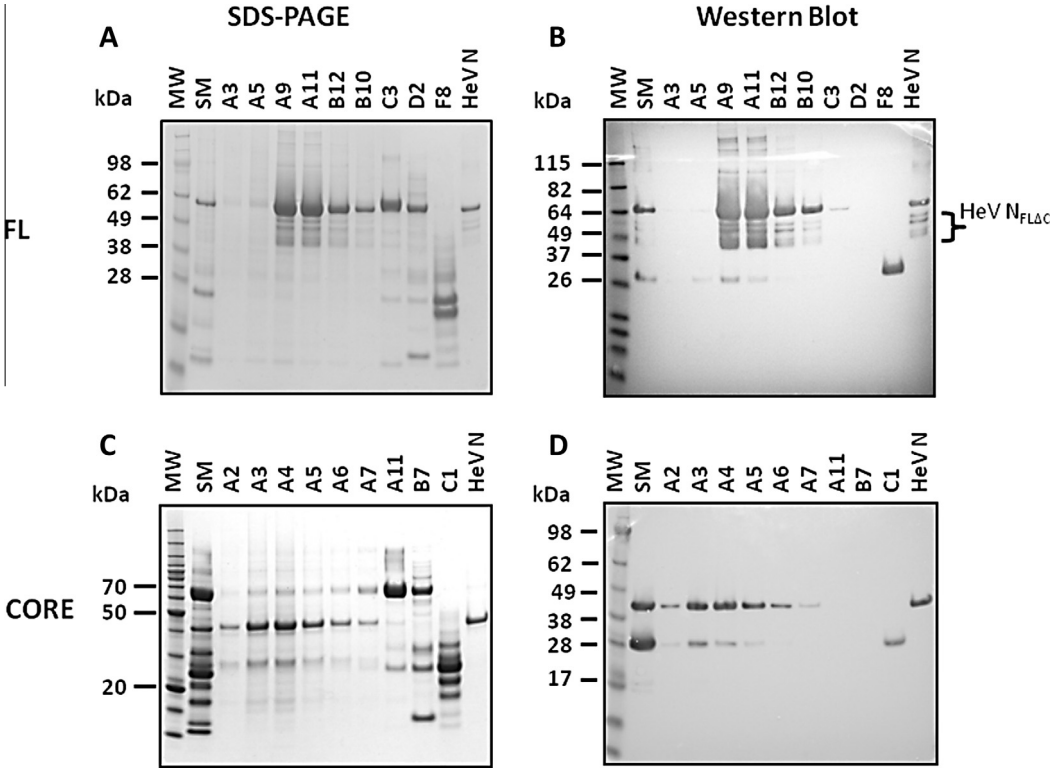

Fig. 4. SDS PAGE and Western analysis of preparative size exclusion chromatography of IMAC purified HeV N constructs. SDS–PAGE analysis of the main peak fractions from SEC of HeV N_{FL} (A) and HeV N_{CORE} (C) on a 4–12% Bis–Tris NuPAGE gradient gel in MES electrophoresis running buffer stained with Coomassie Brilliant Blue R-250. Western blot analysis of fractions post SEC purified HeV N_{FL} (B) and HeV N_{CORE} (D) probed with an anti-His-horseradish peroxidase monoclonal antibody conjugate ((Sigma–Aldrich A7058) 1/2000 in 5% Blotto). His_{x6}-tagged HeV N_{FL} and HeV N_{CORE}, previously purified under the same conditions as described in the manuscript were included as positive controls. HeV $N_{FL\Delta C}$ – C terminal truncated forms of HeV N_{FL}.

concentrator with a 10,000 Da concentrating membrane without protein precipitation or aggregation occurring. We obtained lower yields for HeV N_{CORE}; with 2.0 mg purified from 6 × 1.0 L cultures in 2.5 L shake flasks with a yield of 0.35 mg/L of culture. The purified HeV N_{CORE} could only be concentrated to approximately 0.3 mg/mL before precipitating out of solution.

3.2. Mass spectroscopy

A mass of 63339.8 Da was observed for recombinant HeV N_{FL} by ESI-TOF-MS.

This value was very close to the theoretical mass of 63339.4 Da, and was within the measureable experimental error attributed to the instrument. Purified HeV N_{CORE} had a mass of 46453.7 Da, obtained by ESI-TOF-MS, which was 130 Da less than the expected mass of 46584.4 Da. The resultant difference could be attributed to the loss of a methionine residue from the N-terminus of the protein.

3.3. Electron microscopy

Negative stain TEM analysis of recombinant HeV N_{FL} and HeV N_{CORE} was used to demonstrate their inherent property to spontaneously self-assemble and form helical chains of nucleocapsid proteins in the presence of heterologous nucleic acids.

The HeV N helical-like particles displayed similar widths but formed stacks of variable lengths (Fig. 5). The width of individual particles were measured and averaged; HeV N_{FL} particles (Fig. 5A(a)) was found to have a width of 20.6 ± 2.4 nm (n = 46) and a central dark hollow pore with a diameter of approximately 6.83 ± 1 nm (n = 31); the HeV N_{CORE} particles (Fig. 5B(b)) had similar dimensions with a width of 21.9 ± 1.97 nm (n = 19) and a central pore diameter of approximately 6.5 ± 0.86 nm (n = 16).

3.4. Functional activity of recombinant HeV N_{FL} and HeV N_{CORE}

The antigenic recognition of these recombinant HeV N proteins to antibodies present in serum samples from animals and humans infected with either HeV or NiV through either natural or laboratory acquired infections as well as vaccinated and immunized animals were measured using a Luminex bead-based assay that is capable of detecting multiple analytes in a single assay.

3.5. Luminex assay

An indirect bead-based assay was developed for testing reactivity of HeV N to a range of naturally infected or laboratory infected animal sera. The bead-based assay used in this study was based on Luminex technology and was similar to the binding assay described previously for HeV and NiV sG [32,33]. The multiplexed Luminex assays included both, HeV N_{FL} and HeV N_{CORE} in addition to sG from HeV, NiV and CedPV. A number of different antisera were tested to determine the reactivity and specificity towards each protein (Fig. 6). Animals infected either naturally or in the laboratory showed significant serological response to both forms of HeV N as well as the sG proteins for NiV and HeV but were negative for the closely related henipavirus, CedPV. Most of the normal non-immune sera from non-infected animals and humans displayed minimal reactivity to the HeV N proteins; however, there was some low level reactivity with both antigens to the vaccinated horse sera at both day 0 and day 42, neither of which would be expected to show specific reactivity. There was also some low level reactivity of normal pig and human sera with the HeV N_{CORE} protein.

4. Discussion

There are many reports on the expression of full-length or truncated constructs of NiV N [23,31,34–36], however, there have only been limited studies on the production of recombinant, full-length HeV N [34,36]. In this report, we describe the expression and purification of soluble full-length HeV N (HeV N_{FL}) and a C-terminal truncated core domain (HeV N_{CORE}) lacking the IDR using a bacterial expression systems. Size exclusion chromatography analysis of both HeV N_{FL} and HeV N_{CORE} suggest they are able to self-assemble into high order oligomeric complexes, possibly aided by the presence of bacterial nucleic acid which is acting as a substitute for viral RNA when these proteins are expressed in *E. coli*.

The SDS–PAGE, Western blotting and chromatographic analyses have shown that it is possible to express and purify from *E. coli* soluble HeV N for bead-based immune-assays and electron microscopy studies. Analysis of our expression results have indicated that the expression levels of the two HeV N constructs was significantly different. The C-terminally truncated HeV N_{CORE} construct was expressed at levels at least 30% lower than HeV N_{FL}. We have attempted to improve the expression levels and the solubility level of the HeV N_{CORE} construct by changing the expression media to TB and reducing the expression temperature to 18 °C. The expression level and solubility of a truncated version of the HeV N protein; HeV $N_{CORE(1–399)}$ in *Saccharomyces cerevisiae* has also been reported to be lower than the full-length construct [34]. This observation is also consistent with the results for the expression of the homologous NiV N in *E. coli* from other studies [23].

Transmission electron microscopy studies on negative stained images of *E. coli* expressed HeV N_{FL} and HeV N_{CORE} reveal they have retained the ability to self-assemble into herringbone-like structures in the absence of both viral RNA and viral proteins. Similar observations have previously been made for NiV N expressed in *E. coli* and negative stain EM analysis indicated the presence of nucleocapsid-like herringbone particles of different lengths, morphologically resembling the structure of RNPs isolated from virus particles [23,37]. EM analysis of HeV and NiV N expressed in *S. cerevisiae* also demonstrated that these proteins are able to form nucleocapsid-like herringbone structures and rings [34]. Detailed biophysical characterization studies have been undertaken on the N protein of another paramyxovirus, Measles virus (MeV) [38–40]. Full-length MeV N protein (MeV N_{FL}) was expressed and purified from *E. coli*, C-terminally truncated MeV N (MeV N_{CORE}) was prepared by limited proteolysis [38]. Negative-stain EM studies on these proteins revealed that MeV N_{CORE} polymerizes into very long and extremely rigid helices [29,38], similar to the structures we observed for our HeV N_{CORE}. Interestingly, their studies demonstrated that MeV N_{FL} protein assembled into short and much less rigid helices or mostly only ring structures as we also observed with the HeV N_{FL} images. They postulated that the intrinsically disordered C-terminal tail was responsible for the restricted of polymerization N monomers in full length N proteins [38].

Analysis of the amino acid sequences of both the HeV and NiV N reveal that they do not contain any cysteine residues and subsequently disulfide bonds cannot be responsible for maintaining the tertiary structure of the protein complex. This suggests that the oligomerization of the paramyxovirus N protein is maintained by intra- or intermolecular, non-covalent bonds or by the viral or host expression system nucleic acids (RNA and DNA) or both [23,41,42]. Amino acid alignments identified four highly conserved hydrophobic regions in *Paramyxoviridae* N proteins [43]. The construction of a series of amino acid deletion mutants has enabled the identification of four small continuous stretches of amino acids responsible for the self-assembly of the N protein [37]. The

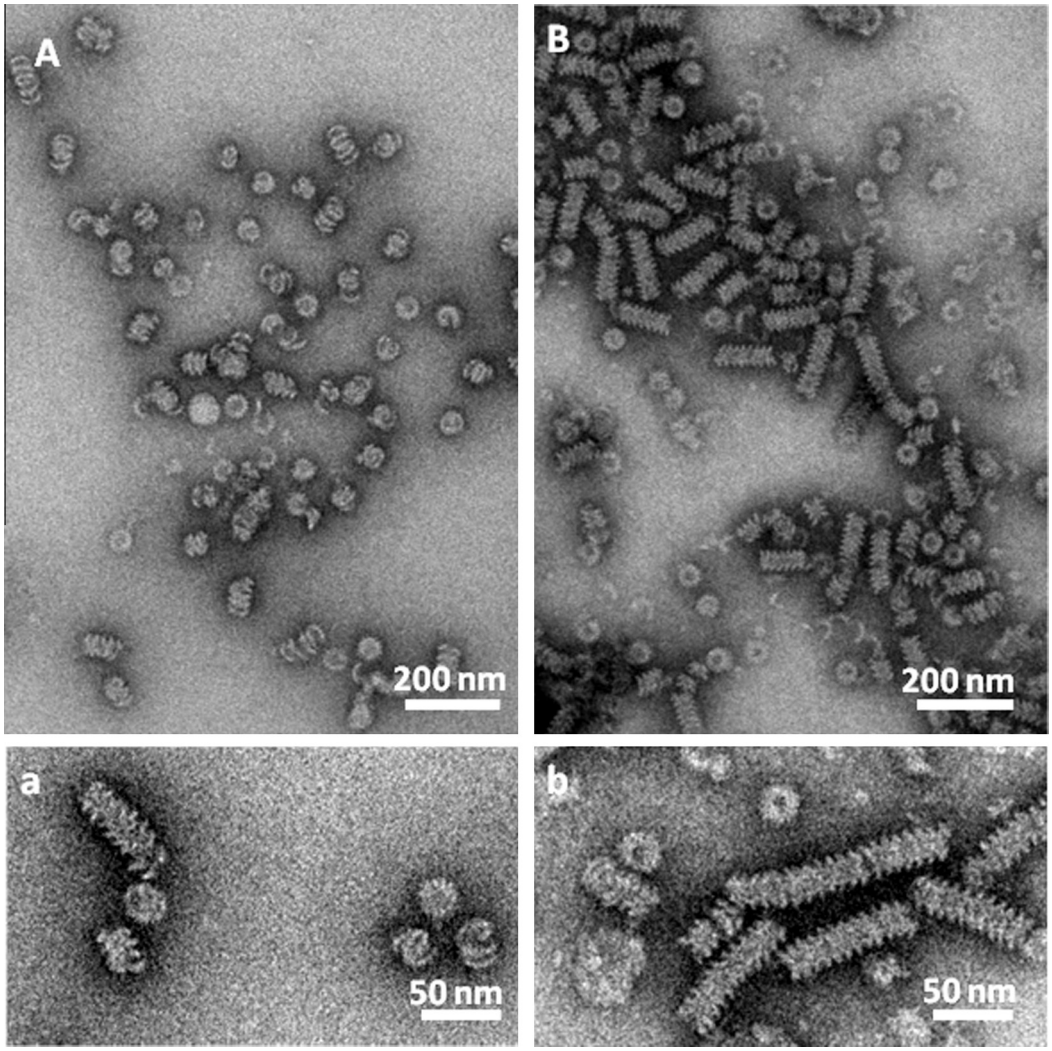

Fig. 5. Transmission electron micrographs of recombinant HeV N_{FL} and HeV N_{CORE}. Electron micrographs of recombinant HeV N_{FL} (A, a) and HeV N_{CORE} (B, b), negatively-stained with 2% phosphotungstic acid. Scale bars are 200 nm (A, B), and 50 nm (a, b) respectively.

removal of any of these domains prevented oligomerization of N monomers; however, the replacement of these deleted regions with the same conserved amino acid region from Newcastle Disease Virus N protein restored oligomerization [37]. These studies further demonstrated that the deletion of more than 129 amino acids from the C-terminus of the NiV N protein inhibited the formation of herringbone-like capsid molecules (NiV $N_{(1-402)}$ and NiV $N_{(1-401)}$), whereas the deletion of less than 128 amino acids did not prevent oligomerization or capsid formation (NiV $N_{(1-404)}$) [37]. Contrary to those observations, our results indicated that HeV $N_{CORE(1-402)}$ is able to still able to form oligomers even with the deletion 130 amino acids, indicating the construct contains all the necessary amino acid residues for self-assembly. Detailed biophysical validation techniques such as analytical ultracentrifugation and multi-angle light scattering are needed to confirm whether HeV N_{FL} and HeV N_{CORE} exist as a stable multimer in solution.

The N proteins from other paramyxovirus, notably Measles virus (MeV) have been studied extensively, the C-terminal tail region has been observed to be extremely sensitive to trypsin digestion, leaving a protease-resistant N-terminal core region of approximately 43 kDa [29]. Further studies on MeV N protein have indicated that the hypervariable C-terminal tail appears to be at the surface of the N assembly with a structure that is not well-visualized by electron microscopy [38,39]. This observation is also a potential indicator that the accessibility of the C-terminal tail region increases the susceptibility of the domain to proteolysis and likelihood of intracellular proteolysis when over-expressed in *E. coli* or other heterologous expression systems. These observations have been made for preparations of HeV N_{FL} protein and NiV N_{FL} expressed in *E. coli* and *S. cerevisiae* [34,35,44,45]. Utilizing bioinformatics proteolysis prediction tools, it has been demonstrated that the proteolytic degradation of *E. coli* expressed NiV N could be reduced by the choice and concentration of specific serine protease inhibitors [35]. Our bacterial expression studies reveal a high level of proteolysis in the *E. coli* preparations of HeV N_{FL}, despite the addition of an extensive cocktail of general and serine specific protease inhibitors to the cellular lysis buffer.

The N protein is the most abundant protein detected in infected cells; amino acid sequence alignments of NiV and HeV $N_{FL(1-532)}$ indicate 92% sequence identity [11]. The $N_{CORE(1-402)}$ region of HeV and NiV is highly conserved (97% sequence homology), whereas the C-terminal tail is more variable, (75% sequence homology). It has been reported for other paramyxoviruses that the C-terminal tail region of the N protein harbors the majority of the antigenic epitopes [46]. The high level of sequence homology between the HeV and NiV N indicates that the HeV N is potentially a valuable antigenic reagent to enable the identification of

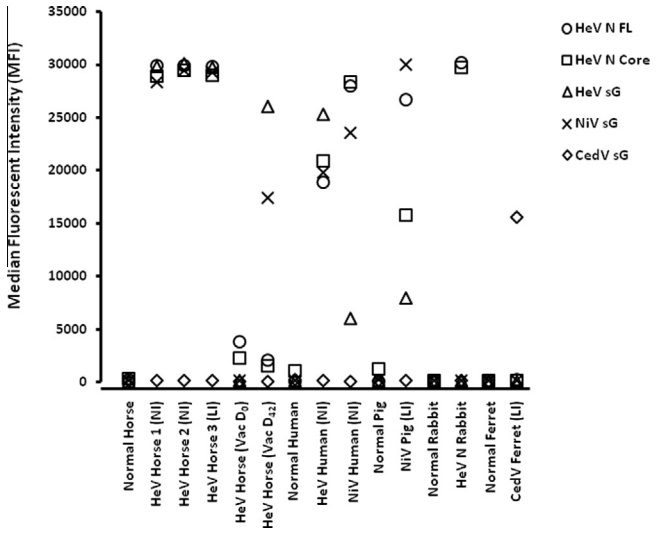

Fig. 6. Immunoreactivity of recombinant henipavirus nucleocapsid protein and soluble glycoprotein towards different anti-sera from infected and non-infected organisms in a Luminex bead-based assay. Detection of antibodies to recombinant henipavirus N and sG proteins in sera from animals and humans infected naturally (NI) or laboratory infected (LI) with, either HeV, NiV or CedPV, and horses receiving Equivac®HeV vaccine (Vac). Non-infected humans and animals were designated normal. HeV N_{FL} and HeV N_{CORE} together HeV, NiV and CedPV sG were coupled to individual sets of Luminex beads. Binding of specific antibodies were detected using biotinylated Protein A and biotinylated Protein G and streptavidin–phycoerythrin. The results were recorded as the Mean Fluorescent Intensity (MFI) of 100 beads.

potential animal hosts carrying either HeV or NiV serum antibodies which may or may not present acute symptoms following henipavirus infection.

The Luminex bead-based fluorescent microsphere assay has been developed for antibody detection and differentiation of HeV and NiV [33], using a method described previously [32]. One of the complications with Luminex bead-based detection assay is the requirement for highly-purified and correctly folded proteins. The Luminex assay results from this study indicate that bacterially-expressed HeV N appear to provide both the purity and the quality of reagent suitable for the Luminex multiplex format, as both forms of the HeV N protein investigated are recognized by serum antibodies from animals or humans infected with either HeV or NiV.

The release of the HeV horse vaccine (Equivac®) presents a significant challenge for diagnosis of natural HeV infections in the field. The current assays utilize the vaccine antigen (HeV sG) and as such are unable to differentiate infected from vaccinated animals (DIVA). The gold standard diagnostic assay is the virus neutralization test which is also ineffective in determining if an animal has been infected or vaccinated. The Luminex assay results from this study indicate that either format of recombinant HeV N expressed and purified could be used equally well to detect antibodies in HeV-infected animals, as well as those infected with the closely related NiV, but are able to differentiate from other known henipaviruses (Cedar Virus (CedPV)), providing an important component of a DIVA assay. The low-level immunoreactivity seen with the HeV N_{CORE} to normal horse, vaccinated horse, normal human and normal pig and to the vaccinated horse sera for the HeV N_{FL} is most likely due to cross-reactivity to related paramyxoviruses, since the N protein of paramyxoviruses is highly conserved. There has only been limited optimization of the antigen coupling process in this assay and further adjustment may also increase the differentiation of positive and negative HeV sera lowering the threshold for negative sera. These proteins would need to be tested against large numbers of normal sera and against control sera for other paramyxoviruses to determine the levels of cross reactivity prior to their validation in DIVA assays. Despite this low-level reactivity, the promising results from the Luminex assay indicate that both forms of recombinant HeV N would be valuable antigens to differentiate animals which had been naturally infected with HeV from those vaccinated with the HeV soluble Glycoprotein (sG) vaccine. Additionally, they will also be valuable reagents for serological surveillance of henipaviruses in wildlife and domestic livestock when used along with the sG in multiplex assays. When used in combination they will provide an opportunity for the identification of antibodies to related viruses that would otherwise be missed by the specificity of the sG proteins.

5. Conclusions

We have successfully over-expressed and purified soluble recombinant HeV N_{FL} and HeV N_{CORE} using a bacterial expression system without the need of a solubility tag or fusion partner. Both HeV N_{FL} and HeV N_{CORE} form higher order oligomers as demonstrated by SEC and negative-stain TEM. Furthermore, monitoring the SEC profile at A_{260} demonstrated that the higher order oligomers of both the HeV N_{FL} and HeV N_{CORE} retained the ability to bind *E. coli* nucleic acids *in vitro*, immunoblots with the anti-His_{x6} antibody confirmed that the proteins in these peaks were HeV N. TEM analysis revealed both forms of HeV N assembled into helical ring-like structures that very closely resembled paramyxovirus-like particles Using a Luminex bead-based immunoassay, we were able to demonstrate both recombinant HeV N_{FL} and HeV N_{CORE} were highly immuno-reactive towards sera from animals and humans infected with either HeV or its' very close relative, NiV, but not with sera from animals infected with a non-pathogenic Henipavirus, CedPV. Furthermore, by incorporating this antigen into the current assays we are now able to distinguish between animals infected with HeV (or NiV) and those vaccinated against this virus. The ability to identify infected from vaccinated animals will be a very useful tool for undertaking epidemiological studies and understanding infection and transmission dynamics of HeV between its' natural host reservoir pteropid bats and spillover targets domestic livestock and humans. The availability of correctly folded recombinant HeV N proteins, will also allow us to enhance the rapid, specific, and ultra-sensitive detection systems that do not require the use of live virus for detecting specific HeV antibodies in virus neutralization assays.

Author contribution

L.A.P., M.Y., L.J.W., J.A.B., J.A.S., G.S.C and W.J.M. designed and performed the experiments. L.A.P., M.Y., G.S.C. and W.J.M. analyzed the data and wrote the manuscript.

Conflict of interest

All the authors declare no competing financial, personal or other relationships with other people or organizations that could inappropriately influence, or be perceived to influence, the research within this study.

Submission declaration and verification

All authors declare that; the work described within this manuscript has not been published previously and is not under consideration for publication elsewhere, that its publication is approved by all authors and tacitly or explicitly by the responsible authorities where the studies were carried out, and that, if

accepted, it will not be published elsewhere in the same form, in English or in any other language, including electronically without the written consent of the copyright-holder.

Acknowledgements

This work was supported by funding from CSIRO Materials Science and Engineering Capability Development Fund and CSIRO Transformational Biology Capability Platform for enhancing recombinant protein production (WM). We thank Dr. Lindsay Sparrow, CSIRO Manufacturing Flagship for performing the mass spectroscopy analysis, Kaylene Selleck for technical assistance, Dr. Yonggang Zhu and Dr. Greg Coia (CSIRO Manufacturing Flagship) for project management and Dr. Timothy Adams (CSIRO Manufacturing Flagship) for critically reading this manuscript and helpful discussions.

References

[1] K.E. Jones, N.G. Patel, M.A. Levy, A. Storeygard, D. Balk, J.L. Gittleman, P. Daszak, Global trends in emerging infectious diseases, Nature 451 (2008) 990–994, http://dx.doi.org/10.1038/nature06536.

[2] A.D. Luis, D.T.S. Hayman, T.J.O. Shea, P.M. Cryan, A.T. Gilbert, R.C. Juliet, J.N. Mills, M.E. Timonin, C.K.R. Willis, A.A. Cunningham, R. Anthony, C.E. Rupprecht, J.L.N. Wood, C.T. Webb, J.R.C. Pulliam, R. Fooks, A comparison of bats and rodents as reservoirs of zoonotic viruses: are bats special?, Proc. R. Soc. B 280 (2013) 1–9.

[3] J.R.C. Pulliam, J. Dushoff, Ability to replicate in the cytoplasm predicts zoonotic transmission of livestock viruses, J. Infect. Dis. 199 (2009) 565–568, http://dx.doi.org/10.1086/596510.

[4] H. Field, P. Young, J.M. Yob, J. Mills, L. Hall, J. Mackenzie, The natural history of Hendra and Nipah viruses, Microbes Infect. 3 (2001) 307–314 (<http://www.ncbi.nlm.nih.gov/pubmed/11334748>).

[5] J.L.N. Wood, M. Leach, L. Waldman, H. Macgregor, A.R. Fooks, K.E. Jones, O. Restif, D. Dechmann, D.T.S. Hayman, K.S. Baker, A.J. Peel, A.O. Kamins, J. Fahr, Y. Ntiamoa-Baidu, R. Suu-Ire, R.F. Breiman, J.H. Epstein, H.E. Field, et al., A framework for the study of zoonotic disease emergence and its drivers: spillover of bat pathogens as a case study, Philos. Trans. R. Soc. Lond. B Biol. Sci. 367 (2012) 2881–2892, http://dx.doi.org/10.1098/rstb.2012.0228.

[6] C.H. Calisher, J.E. Childs, H.E. Field, K.V. Holmes, T. Schountz, Bats: important reservoir hosts of emerging viruses, Clin. Microbiol. Rev. 19 (2006) 531–545, http://dx.doi.org/10.1128/CMR.00017-06.

[7] L.A. Selvey, R.M. Wells, J.G. McCormack, A.J. Ansford, K. Murray, R.J. Rogers, P.S. Lavercombe, P. Selleck, J.W. Sheridan, Infection of humans and horses by a newly described morbillivirus, Med. J. Aust. 162 (1995) 642–645. (http://www.ncbi.nlm.nih.gov/pubmed/7603375).

[8] B.T. Eaton, C.C. Broder, D. Middleton, L.-F. Wang, Hendra and Nipah viruses: different and dangerous, Nat. Rev. Microbiol. 4 (2006) 23–35, http://dx.doi.org/10.1038/nrmicro1323.

[9] M. Aljofan, Hendra and Nipah infection: emerging paramyxoviruses, Virus Res. 177 (2013) 119–126, http://dx.doi.org/10.1016/j.virusres.2013.08.002.

[10] M. Enserink, New virus fingered in Malaysian epidemic, Science 284 (1999) 407–410, http://dx.doi.org/10.1126/science.284.5413.407.

[11] B.H. Harcourt, A. Tamin, T.G. Ksiazek, P.E. Rollin, L.J. Anderson, W.J. Bellini, P.A. Rota, Molecular characterization of Nipah virus, a newly emergent paramyxovirus, Virology 271 (2000) 334–349, http://dx.doi.org/10.1006/viro.2000.0340.

[12] K.L. Sai, B.C. Kaw, Nipah virus encephalitis outbreak in Malaysia, Clin. Infect. Dis. 34 (2002) S48–S51, http://dx.doi.org/10.1086/338818.

[13] J.N. Mills, A.N.M. Alim, M.L. Bunning, O.B. Lee, K.D. Wagoner, B.R. Amman, P.C. Stockton, T.G. Ksiazek, Nipah virus infection in dogs, Malaysia, 1999, Emerg. Infect. Dis. 15 (2009) 950–952, http://dx.doi.org/10.3201/eid1506.080453.

[14] G.A. Marsh, C. de Jong, J.A. Barr, M. Tachedjian, C. Smith, D. Middleton, M. Yu, S. Todd, A.J. Foord, V. Haring, J. Payne, R. Robinson, I. Broz, G. Crameri, H.E. Field, L.F. Wang, Cedar virus: a novel henipavirus isolated from Australian bats, PLoS Pathog. 8 (2012) 1–11, http://dx.doi.org/10.1371/journal.ppat.1002836.

[15] L.-F. Wang, P. Daniels, Diagnosis of henipavirus infection: current capabilities and future directions, in: B. Lee, A. Rota, Paul (Eds.), Current Topics in Microbiology and Immunology, Springer, 2012, pp. 179–196.

[16] J. Pallister, D. Middleton, L.-F. Wang, R. Klein, J. Hanning, R. Robinson, M. Yamada, J. White, J. Payne, Y.-R. Feng, Y.-P. Chan, C.C. Broder, A recombinant Hendra virus G glycoprotein-based subunit vaccine protects ferrets from lethal Hendra virus challenge, Vaccine 29 (2011) 5623–5630, http://dx.doi.org/10.1016/j.vaccine.2011.06.015.A.

[17] J.A. Pallister, R. Klein, R. Arkinstall, J. Haining, F. Long, J.R. White, J. Payne, Y.-R. Feng, L.-F. Wang, C.C. Broder, D. Middleton, Vaccination of ferrets with a recombinant G glycoprotein subunit vaccine provides protection against Nipah virus disease for over 12 months, Virol. J. 10 (2013) 237–244, http://dx.doi.org/10.1186/1743-422X-10-237.

[18] C.C. Broder, K. Xu, D.B. Nikolov, Z. Zhu, D.S. Dimitrov, D. Middleton, J. Pallister, T.W. Geisbert, K.N. Bossart, L.F. Wang, A treatment for and vaccine against the deadly Hendra and Nipah viruses, Antiviral Res. 100 (2013) 8–13, http://dx.doi.org/10.1016/j.antiviral.2013.06.012.

[19] L. Wang, M. Yu, E. Hansson, L.I. Pritchard, B. Shiell, W.P. Michalski, B.T. Eaton, The exceptionally large genome of Hendra virus: support for creation of a new genus within the family Paramyxoviridae, J. Virol. 74 (2000) 9972–9979, http://dx.doi.org/10.1128/JVI.74.21.9972-9979.2000.Updated.

[20] M.K. Lo, A. Rota, Paul, Molecular virology of henipaviruses, in: B. Lee, A. Rota, Paul (Eds.), Current Topics in Microbiology and Immunology, Springer, 2012, pp. 41–58.

[21] J. Habchi, S. Longhi, Structural disorder within paramyxovirus nucleoproteins and phosphoproteins, Mol. BioSyst. 8 (2012) 69–81, http://dx.doi.org/10.1039/c1mb05204g.

[22] M. Huang, H. Sato, K. Hagiwara, A. Watanabe, A. Sugai, F. Ikeda, H. Kozuka-Hata, M. Oyama, M. Yoneda, C. Kai, Determination of a phosphorylation site in Nipah virus nucleoprotein and its involvement in virus transcription, J. Gen. Virol. 92 (2011) 2133–2141, http://dx.doi.org/10.1099/vir.0.032342-0.

[23] W.S. Tan, S.T. Ong, M. Eshaghi, S.-S. Foo, K. Yusoff, Solubility, immunogenicity and physical properties of the nucleocapsid protein of Nipah virus produced in *Escherichia coli*, J. Med. Virol. 73 (2004) 105–112, http://dx.doi.org/10.1002/jmv.20052.

[24] P. Hausmann, D. Kolakofsky, T. Pelet, D. Garcin, J. Curran, L. Roux, Minireview Paramyxovirus RNA synthesis and the requirement for hexamer genome length: the rule of six revisited, J. Virol. 72 (1998) 891–899.

[25] D. Vulliémoz, L. Roux, "Rule of Six": how does the Sendai virus RNA polymerase keep count?, J Virol. 75 (2001) 4506–45018, http://dx.doi.org/10.1128/JVI.75.10.4506.

[26] Z. Shi, Emerging infectious diseases associated with bat viruses, Sci. China Life Sci. 56 (2013) 678–682, http://dx.doi.org/10.1007/s11427-013-4517-x.

[27] J.H. Kuhn, S. Becker, H. Ebihara, T.W. Geisbert, K.M. Johnson, Y. Kawaoka, W.I. Lipkin, A.I. Negredo, S.V. Netesov, S.T. Nichol, G. Palacios, C.J. Peters, A. Tenorio, V.E. Volchkov, P.B. Jahrling, Proposal for a revised taxonomy of the family Filoviridae: classification, names of taxa and viruses, and virus abbreviations, Arch. Virol. 155 (2010) 2083–2103, http://dx.doi.org/10.1007/s00705-010-0814-x.

[28] H. Zhou, Y. Sun, Y. Guo, Z. Lou, Structural perspective on the formation of ribonucleoprotein complex in negative-sense single-stranded RNA viruses, Trends Microbiol. 21 (2013) 475–484, http://dx.doi.org/10.1016/j.tim.2013.07.006.

[29] G. Schoehn, M. Mavrakis, A. Albertini, R. Wade, A. Hoenger, R.W.H. Ruigrok, The 12 Å structure of trypsin-treated measles virus N-RNA, J. Mol. Biol. 339 (2004) 301–312, http://dx.doi.org/10.1016/j.jmb.2004.03.073.

[30] M. Yu, E. Hansson, B. Shiell, W. Michalski, B.T. Eaton, L.-F. Wang, Sequence analysis of the Hendra virus nucleoprotein gene: comparison with other members of the subfamily Paramyxovirinae, J. Gen. Virol. 79 (1998) 1775–1780.

[31] Y.P. Chan, C.L. Koh, S.K. Lam, L.-F. Wang, Mapping of domains responsible for nucleocapsid protein-phosphoprotein interaction of henipaviruses, J. Gen. Virol. 85 (2004) 1675–1684, http://dx.doi.org/10.1099/vir.0.19752-0.

[32] K.N. Bossart, J.A. McEachern, A.C. Hickey, V. Choudhry, D.S. Dimitrov, B.T. Eaton, L.-F. Wang, Neutralization assays for differential henipavirus serology using Bio-Plex protein array systems, J. Virol. Methods 142 (2007) 29–40, http://dx.doi.org/10.1016/j.jviromet.2007.01.003.

[33] L. McNabb, J. Barr, G. Crameri, S. Juzva, S. Riddell, A. Colling, V. Boyd, C. Broder, L.-F. Wang, R. Lunt, Henipavirus microsphere immuno-assays for detection of antibodies against Hendra virus, J. Virol. Methods 200 (2014) 22–28, http://dx.doi.org/10.1016/j.jviromet.2014.01.010.

[34] M. Juozapaitis, A. Serva, A. Zvirbliene, R. Slibinskas, J. Staniulis, K. Sasnauskas, B.J. Shiell, L.-F. Wang, W.P. Michalski, Generation of henipavirus nucleocapsid proteins in yeast *Saccharomyces cerevisiae*, Virus Res. 124 (2007) 95–102, http://dx.doi.org/10.1016/j.virusres.2006.10.008.

[35] F.C. Chong, W.S. Tan, D.R.A. Biak, T.C. Ling, B.T. Tey, Modulation of protease activity to enhance the recovery of recombinant nucleocapsid protein of Nipah virus, Process Biochem. 45 (2010) 133–137, http://dx.doi.org/10.1016/j.procbio.2009.08.012.

[36] C. Xiao, Y. Liu, Y. Jiang, D.E. Magoffin, H. Guo, H. Xuan, G. Wang, L.-F. Wang, C. Tu, Monoclonal antibodies against the nucleocapsid proteins of henipaviruses: production, epitope mapping and application in immunohistochemistry, Arch. Virol. 153 (2008) 273–281, http://dx.doi.org/10.1007/s00705-007-1079-x.

[37] S.T. Ong, K. Yusoff, C.L. Kho, J.O. Abdullah, W.S. Tan, Mutagenesis of the nucleocapsid protein of Nipah virus involved in capsid assembly, J. Gen. Virol. 90 (2009) 392–397, http://dx.doi.org/10.1099/vir.0.005710-0.

[38] S. Longhi, V. Receveur-Bréchot, D. Karlin, K. Johansson, H. Darbon, D. Bhella, R. Yeo, S. Finet, B. Canard, The C-terminal domain of the measles virus nucleoprotein is intrinsically disordered and folds upon binding to the C-terminal moiety of the phosphoprotein, J. Biol. Chem. 278 (2003) 18638–18648, http://dx.doi.org/10.1074/jbc.M300518200.

[39] M.R. Jensen, G. Communie, E.A. Ribeiro, N. Martinez, A. Desfosses, L. Salmon, L. Mollica, F. Gabel, M. Jamin, S. Longhi, R.W.H. Ruigrok, M. Blackledge, Intrinsic disorder in measles virus nucleocapsids, Proc. Natl. Acad. Sci. U.S.A. 108 (2011) 9839–9844, http://dx.doi.org/10.1073/pnas.1103270108.

[40] I. Gutsche, A. Desfosses, G. Effantin, W.L. Ling, M. Haupt, R.W.H. Ruigrok, C. Sachse, G. Schoehn, Near-atomic cryo-EM structure of the helical measles virus nucleocapsid, Science 348 (2015) 704–707, http://dx.doi.org/10.1126/science.aaa5137.

[41] M. Eshaghi, W.S. Tan, S.T. Ong, K. Yusoff, Purification and characterization of Nipah virus nucleocapsid protein produced in insect cells, J. Clin. Microbiol. 43 (2005) 3172–3177, http://dx.doi.org/10.1128/JCM.43.7.3172.

[42] F. Ferron, Z. Li, I. Danek, Eric, D. Luo, Y. Wong, B. Coutard, V. Lantez, R. Charrel, B. Canard, T. Walz, J. Lescar, The hexamer structure of the Rift Valley fever virus nucleoprotein suggests a mechanism for its assembly into ribonucleoprotein complexes, PLoS Pathog. 7 (2011) 1–12, http://dx.doi.org/10.1371/journal.ppat.1002030.

[43] C.L. Kho, W.S. Tan, K. Yusoff, Sequence analysis of the nucleoprotein of a Newcastle disease virus heat resistant strain: comparison with other members of the Paramyxoviridae, J. Biochem. Mol. Biol. Biophys. 5 (2001) 463–471.

[44] F.C. Chong, W.S. Tan, D.R.A. Biak, T.C. Ling, B.T. Tey, Purification of histidine-tagged nucleocapsid protein of Nipah virus using immobilized metal affinity chromatography, J. Chromatogr. B 877 (2009) 1561–1567, http://dx.doi.org/10.1016/j.jchromb.2009.03.048.

[45] J. Habchi, S. Blangy, L. Mamelli, M.R. Jensen, M. Blackledge, H. Darbon, M. Oglesbee, Y. Shu, S. Longhi, Characterization of the interactions between the nucleoprotein and the phosphoprotein of Henipavirus, J. Biol. Chem. 286 (2011) 13583–13602, http://dx.doi.org/10.1074/jbc.M111.219857.

[46] K.W. Ryan, A. Portner, K.G. Murti, Antibodies to paramyoxovirus nucleoproteins define regions important for immunogenicity and nucleocapsid assembly, Virology 193 (1993) 376–384, http://dx.doi.org/10.1006/viro.1993.1134.